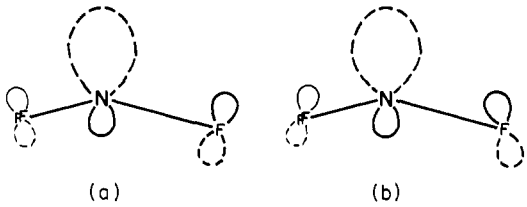

Figure 4. Schematic representation of the two possible local orbital schemes for the highest (singly) occupied molecular orbital in NF_3^+·; (a) F orbital essentially orthogonal to bond direction, $\alpha = +15°$; (b) F orbital tilted toward bond direction, $\alpha = -15°$.

Conclusions

Despite an apparently large, diffuse background, it has been possible to obtain satisfactory Zeeman, nitrogen hyperfine, and fluorine hyperfine matrices for the rigid trigonal-pyramidal $\cdot NF_3^+$ radical cation by computer simulation of the EPR spectra of λ-irradiated NF_4AsF_6 and $^{15}NF_4AsF_6$, annealed and then cooled to ~25 K.

All the data can be rationalized in terms of a hybrid-orbital bonding scheme with (1) the unpaired electron in mainly a nonbonding N($sp^{6.35}$) orbital (which also to some extent involves fluorine p_z orbitals in an antibonding interaction), (2) $sp^{2.5}$ nitrogen hybrid bonding orbitals, (3) 105° angles between the threefold axis and the N–F bonds, and (4) the fluorine part of the HOMO being mainly p_z-like, with its z axis tilted plus or minus 15° from the threefold axis (see Figure 4).

The isoelectronic radical $\cdot CF_3$ is similar, the corresponding angle being 108° and the carbon bonding hybrids about sp^3 (see Table II). Unfortunately, no anisotropic data are available for BF_3^-, the next member of the isoelectronic series; isotropic parameters are compared in Table II.

The structural angles between the C_3 axis and normals to the bonds for $\cdot NF_3^+$ and $\cdot CF_3$ are ~14.6° and 19.6°, respectively. The principal axes of the fluorine hyperfine matrices deviate from the C_{3v} axes by ~15° and 18°, respectively. Depending on the sign of this deviation, these fluorine A axes could be either essentially perpendicular to or tilted, by ~30° or 37°, respectively, from the N–F or C–F bonds. The latter interpretation (schematically indicated in Figure 4b) is supported by electronic structure calculations.

Acknowledgment. This work was in part supported by the National Science Foundation Quantum Chemistry Program, the U.S. Army Research Office, and the Office of Naval Research. We thank Mary Kolor Gurnick for helpful suggestions.

Registry No. $^{14}NF_3^+$·, 54384-83-7; $^{15}NF_3^+$·, 67745-75-9; NF_4AsF_6, 16871-75-3.

Ab Initio SCF Study of Hyperfine Couplings, Geometries, and Inversion Barriers in the Isoelectronic Radicals NF_3^+, CF_3, and BF_3^-

M. A. Benzel, A. M. Maurice, R. L. Belford,* and C. E. Dykstra*

Contribution from the School of Chemical Sciences, University of Illinois, Urbana, Illinois 61801. *Received April 26, 1982*

Abstract: Ab initio SCF molecular orbital calculations with double-ζ and polarized double-ζ bases are reported for the isoelectronic series of C_{3v} radicals $\cdot NF_3^+$, $\cdot CF_3$, and $\cdot BF_3^-$. At the potential minima, the bond lengths are 1.314 Å for NF_3^+, 1.341 Å for CF_3, and 1.442 Å for BF_3^-; the complements of the umbrella angles are +12.1° for NF_3^+, +17.1° for CF_3, and +19.6° for BF_3^-. Calculated inversion barriers are about 11, 33, and 28 kcal/mol for NF_3^+, CF_3, and BF_3^-, respectively. Bonding and the predicted dependence of EPR parameters upon radical geometry are discussed. With respect to the spin-density distribution and the radical geometry, these calculations confirm the general inferences drawn from the previous EPR analysis—in particular, the hyperfine interaction of the central atom. However, an experimental ambiguity in orientation of the principal axis of the fluorine hyperfine coupling matrix is resolved in favor of the nonintuitive alternative. It is concluded that quantitative information about the geometry of such radicals cannot be inferred from the orientation of the halogen hyperfine axes.

The trigonal-pyramidal fluorocarbon $\cdot CF_3$ and its isoelectric neighbors $\cdot NF_3^+$ and $\cdot BF_3^-$ are archetypal fluoro radicals. However, there have been no direct determinations of the molecular structure of any of these species, and experimental information bearing on their electronic structure is still being accumulated.[1] The most detailed experimental clues available on these species are to be found in the anisotropic electron paramagnetic resonance spectra of $\cdot YM_3$ (Y = C, N^+, B^-) as impurity sites in solids at low temperature. An intriguing feature of both $\cdot CF_3$, whose EPR parameters are fairly well-known, and $\cdot NF_3^+$, for which anisotropic EPR results are just now being reported,[1] is that the angle α between the trigonal axis and the principal axis of the ^{19}F hyperfine coupling tensor is about the same as the structural angle α' by the pyramid is expected to deviate from a planar structure. The obvious interpretation is that the part of the spin density localized on the fluorine center occupies a pπ orbital oriented perpendicular to the bond. However, since the experiments were done on isotropic (polycrystalline) samples, the relative signs of α and α' are indeterminable. If they are of opposite sign, the obvious interpretation is invalid. In that event, it would seem that the fluorine p orbital involved in the highest (singly occupied) molecular orbital would be poised for bonding by being strongly skewed with respect to the Y–F (Y = C, B^-, or N^+) bond. In the case of $\cdot CF_3$, INDO calculations and limited ab initio calculations[2] have supported this second interpretation. Here we report ab initio self-consistent-field (SCF) calculations with large basis sets, caried out to determine not only the equilibrium structures of the three radicals but also their inversion barriers. These calculations provide detailed information on the electron-spin distributions leading to an elucidation of the rela-

(1) A. M. Maurice, R. L. Belford, I. B. Goldberg, and K. O. Christe, *J. Am. Chem. Soc.*, preceding paper in this issue.

(2) O. Edlund, A. Lund, M. Shiotani, J. Sohma, and K. A. Thuomas, *Mol. Phys.*, **32**, 49 (1976).

0002-7863/83/1505-3802$01.50/0

Table I. Calculated Bond Distances in Å

	equilibrium geometry					
	pyramidal			planar		
calcd[a]	$\cdot NF_3^+$	$\cdot CF_3$	$\cdot BF_3^-$	$\cdot NF_3^+$	$\cdot CF_3$	$\cdot BF_3^-$
DZ*	1.314	1.341	1.442	1.312	1.333	1.334
DZ	1.318	1.344	1.455	1.316	1.336	1.447

[a] DZ* and DZ refer to double-ζ-level calculations with and without added diffuse basis functions, respectively.

tionship between α, and α' and the nature of the molecular bonding. The results also provide predictions of EPR parameters for $\cdot BF_3^-$, for which experimental data are fragmentary.

Theoretical Approach

Ab initio spin- and symmetry-restricted self-consistent-field (SCF) calculations were performed on the three isoelectronic systems. Most of the calculations were performed with a (9s5p/4s2p) Dunning contracted[3] double-ζ (DZ) basis of Huzinaga's primitive Gaussian functions.[4] This basis[5] was supplemented with polarization functions[5] ($\alpha_{3d}(B) = 0.7$, $\alpha_{3d}(C) = 0.75$, $\alpha_{3d}(N) = 0.77$, $\alpha_{3d}(F) = 0.9$) in the calculations designated DZ + P. Tests of the importance of diffuse functions were made by supplementing the DZ basis with diffuse s and p functions[5] ($\alpha_{sp}(B) = 0.03$, $\alpha_{sp}(C) = 0.05$, $\alpha_{sp}(N) = 0.06$, $\alpha_{sp}(F) = 0.09$). This basis is designated DZ*.

Complete geometry optimizations to find the equilibrium structures were performed with the DZ and DZ* basis sets. Optimizations were not performed with the DZ + P basis because with the neglect of correlation effects, the inclusion of polarization functions may yield bond-length predictions that are substantially too short.[6] Bond lengths were also optimized with the DZ and DZ* bases under the constraint that the three structures be planar. This optimization determines the saddle point for the pyramidal inversion of the molecules. DZ/SCF calculations were performed at a number of points on the inversion potential surfaces by setting bond lengths at their equilibrium value and choosing various pyramidal angles. In addition, at a few of these chosen angles, bond lengths were optimized to yield geometrical structures that correspond to points on the minimum energy path for the inversion.

Properties were calculated with a program by Gandhi[7a] and spin-density and orbital contours were plotted by use of a program by Jorgensen.[7b] Since the calculations were spin-restricted, the spin density arises only from the singly occupied open-shell orbital, ϕ_{6a_1}. The anisotropic (dipolar) part of the hyperfine coupling interaction for nucleus n was calculated as

$$T_{nab} = g_e\mu_B g_n \int d\tau\, \phi^2 r_n^{-5}(3a_n b_n - r_n^2\delta_{ab})$$

where g_e and g_n are the electronic and nuclear g factors, respectively, μ_B and μ_n are the Bohr and nuclear magnetons, respectively, a_n and b_n are any pair of Cartesian coordinates of the unpaired electron as measured from nucleus n, and r_n is its distance from nucleus n.

Results and Discussion

Geometry and Configuration. For all molecules, the lowest energy conformation was a nonplanar, trigonal pyramid with an orbital occupancy (in C_{3v})

$$1e^4 1a_1^2 2a_1^2 3a_1^2 2e^4 4a_1^2 3e^4 5a_1^2 4e^4 5e^4 1a_2^2 6a_1^1$$

corresponding to a $^2A_1$ ground state. The qualitative description of these molecules as trigonal pyramids is in agreement with the minimal-basis-set results of So,[8] but the predicted bond lengths and angles are significantly different. The planar conformation has a $^2A_1''$ ground state in D_{3h} for $\cdot NF_3^+$ and $\cdot CF_3$ and a $^2A_2''$ ground state for $\cdot BF_3^-$. Tables I and II list the bond distances, bond angles, and umbrella angles. As expected, the addition of diffuse functions to the basis set made very little difference except for the negative ion, $\cdot BF_3^-$. The predicted umbrella angles correspond to almost perfectly tetrahedral bonding for $\cdot BF_3^-$ (the bond angle being 109°), slight flattening for $\cdot CF_3$, and significant flattening for $\cdot NF_3^+$ where the bond angle of 115.7° is about halfway between tetrahedral and perfect trigonal (120°) bonding.

Inversion Barriers. The minimum-energy path for inversion involves small changes in the bond lengths for $\cdot NF_3^+$ and $\cdot CF_3$. The basis set supplemented with diffuse functions changes the predictions of the structural parameters only slightly, contracting the bond lengths by up to about a hundredth of an angstrom. The bond length of the neutral species $\cdot CF_3$ is about 0.03 Å longer than that of the positively charged species $\cdot NF_3^+$. The bond length in $\cdot BF_3^-$ is the longest, being roughly 0.1 Å longer than that of $\cdot CF_3$. At the inversion saddle-point structure, the $\cdot BF_3^-$ bonds contract to lengths comparable with the other species.

The inversion energies given in Table III show sharp differences between the systems. $\cdot NF_3^+$ has the lowest barrier, about 5.5 kcal at the DZ/SCF level. Diffuse functions have little effect, but polarization functions raise this barrier by almost 6 kcal. This is expected since the polarization functions provide more flexibility in describing the orientation of the electron distribution at each atomic center and thus are necessary to properly describe the nonplanar structure. For ammonia, SCF calculations with DZ-quality basis sets but lacking polarization functions have tended to underestimate the inversion barrier or even predict a planar equilibrium structure.[9,10] However, with polarized basis sets, the inversion barrier of ammonia is predicted to within a few tenths of a kcal.[11,12] Comparable polarization-function effects have been found for cyanamide,[14-18] and DZ + P basis calculations[18] on isocyanamide have given structural information in good agreement with the first rotational spectrum results from subsequent experiments.[19]

For $\cdot CF_3$, the inversion barrier is raised from about 26 kcal to about 34 kcal by the inclusion of polarization functions; $\cdot BF_3^-$ shows a smaller difference in the DZ and DZ + P predicted inversion barriers. However, the inclusion of diffuse functions substantially lowers the barrier. Diffuse functions can play a critical role in determining energetics of anions as shown by a number of calculatons[20-24] on the inversion barrier of CH_3^-. These functions allow for the very diffuse character of the central atom's 2p orbital in the planar form; they stabilize the planar structure. The substantial contraction of the BF bond length with diffuse functions indicates their importance in properly describing $\cdot BF_3^-$. Thus, the DZ* result for $\cdot BF_3^-$ is more trustworthy than the DZ result. Taking the polarization-function and diffuse-function effects to be additive yields an estimated barrier of 25–30 kcal. Calculation of this barrier with a DZ* + P basis gives a value

(3) T. H. Dunning, *J. Chem. Phys.*, **53**, 2823 (1970).
(4) S. Huzinaga, *J. Chem. Phys.*, **42**, 1293 (1965).
(5) The DZ basis consists of 40 linearly independent functions per molecule, 4 s type and 6 p type per atom. The diffuse functions add 16 more linearly independent functions per molecule, 1 s type and 3 p type per atom. Polarization adds 24 linearly independent functions per molecule, equivalent to 1 s type and 5 d type per atom.
(6) C. E. Dykstra, *Annu. Rev. Phys. Chem.*, **32**, 25 (1981).
(7) (a) S. Gandhi, University of Illinois Electronic Structure Program No. 6, Urbana IL, 1981; (b) W. L. Jorgensen, *QCPE 10*, **No. 340** (1977).
(8) S. P. So, *J. Chem. Phys.*, **67**, 3929 (1977); *Chem. Phys. Lett.*, **67**, 516 (1979).
(9) A. Veillard, J. M. Lehn, and B. Munsch, *Theor. Chim. Acta.*, **9**, 275 (1968).
(10) U. Kaldor and I. Shavitt, *J. Chem. Phys.*, **45**, 888 (1966).
(11) A. Rauk, L. C. Allen, and E. Clementi, *J. Chem. Phys.*, **52**, 4133 (1970).
(12) R. M. Stevens, *J. Chem. Phys.*, **55**, 1725 (1971).
(13) N. R. Carlsen, L. Radom, N. V. Riggs, and W. R. Rodwell, *J. Am. Chem. Soc.*, **101**, 2233 (1979); W. R. Rodwell and L. Radom, *J. Chem. Phys.*, **72**, 2025 (1980).
(14) J. B. Moffat and C. Vogt, *J. Mol. Spectrosc.*, **33**, 404 (1970).
(15) J. M. Lehn and B. Munsch, *J. Chem. Soc. D*, 1062 (1970).
(16) J. B. Moffat, *J. Mol. Struct.*, **38**, 221 (1977); **52**, 275 (1979).
(17) B. T. Hart, *Aust. J. Chem.*, **26**, 261, 477 (1973).
(18) M. A. Vincent and C. E. Dykstra, *J. Chem. Phys.*, **73**, 3838 (1980).
(19) E. Schäfer, M. Winnewisser, and J. J. *Christiansen, Chem. Phys. Lett.*, **81**, 380 (1981).
(20) A. J. Duke, *Chem. Phys. Lett.*, **21**, 275 (1973).
(21) F. Driessler, R. Ahlrichs, V. Staemmler, and W. Kutzelnigg, *Theor. Chim. Acta*, **30**, 315 (1973).
(22) R. Ahlrichs, H. Lischka, V. Staemmler, and W. Kutzelnigg, *J. Chem. Phys.*, **62**, 1225, 1235 (1975).
(23) D. S. Marynick and D. A. Dixon, *Proc. Natl. Acad. Sci. U.S.A.*, **74**, 410 (1977).
(24) C. E. Dykstra, M. Hereld, R. R. Lucchese, H. F. Schaefer, III, and W. Meyer, *J. Chem. Phys.*, **67**, 4071 (1977).

Table II. Calculated Equilibrium Bond Angles in Degrees

	bond angle, β ($\angle$FMF)			structural angle, α' ($90^\circ - \angle z$MF)			hyperfine angle, α (z to major axis of A_F)		
calcd[a]	$\cdot NF_3^+$	$\cdot CF_3$	$\cdot BF_3^-$	$\cdot NF_3^+$	$\cdot CF_3$	$\cdot BF_3^-$	$\cdot NF_3^+$	$\cdot CF_3$	$\cdot BF_3^-$
DZ*	115.7	111.8	109.3	−12.19	−17.08	−19.60	+18.89	+23.05	+23.40
DZ	115.5	111.6	108.6	−12.43	−17.28	−20.37	+19.17	+23.02	+23.47
DZ/ZO							+19.87	+24.11	+24.26
DZ/OC							+15.91	+19.61	+20.19
EPR	113.9	109.4		−14.6	−19.56		±15.0	±17.8[b]	

[a] DZ* and DZ refer to double-ζ-level calculations with and without added diffuse basis functions, respectively. ZO refers to calculation of properties without inclusion of two-center overlap density. EPR refers to a prediction of bond angle from the ratio of isotropic to anisotropic parts of the central-atom hyperfine coupling matrix; see ref 1. OC refers to calculation of properties with one-center contributions only. [b] Assumed for the analysis. Confirmed by simulations, but error limits unknown.

Table III. Inversion Energies in kcal

	DZ basis	DZ* basis	DZ + P basis[a]
NF_3^+	5.5	5.0	11.1
CF_3	25.9	25.6	33.6
BF_3^-	46.1	22.0	49.5[b]

[a] The geometries obtained by using the DZ basis (see Table I) were used to evaluate the energies with the DZ + P basis. [b] With a DZ* + P basis, the barrier is 28.4 kcal.

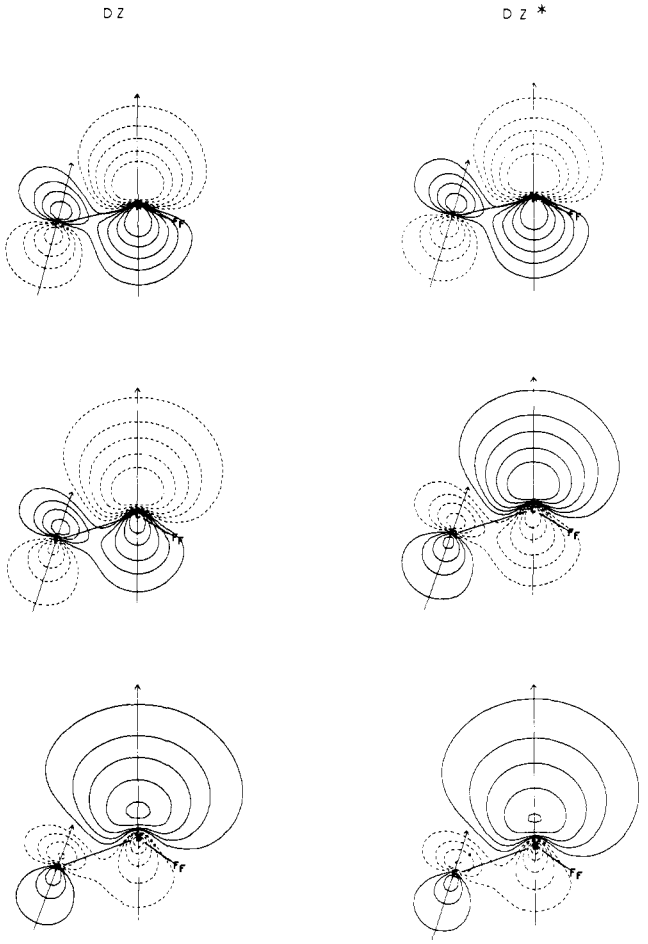

Figure 1. Spin density for $\cdot NF_3^+$, $\cdot CF_3$, $\cdot BF_3^-$, each in its equilibrium configuration. DZ results on left, DZ* on right. Dotted and solid contour lines indicate opposite signs of orbital wave function. Contour levels (going outward) are 0.30, 0.20, 0.12, 0.07, 0.03. Contours are drawn for the xz plane, containing the C_{3v} axis and one MF bond. The other two F nuclei shown are above and below the plane of the paper. The principal axis of the F hyperfine coupling matrix computed from the given spin density is indicated as an arrow on each contour plot.

of 28.4 kcal that is within this range. The role of the diffuse functions for planar BF_3^- is substantial; they are necessary to properly stabilize the half-filled a_2'' orbital. Without them, an a_1'' orbital is lower in energy.

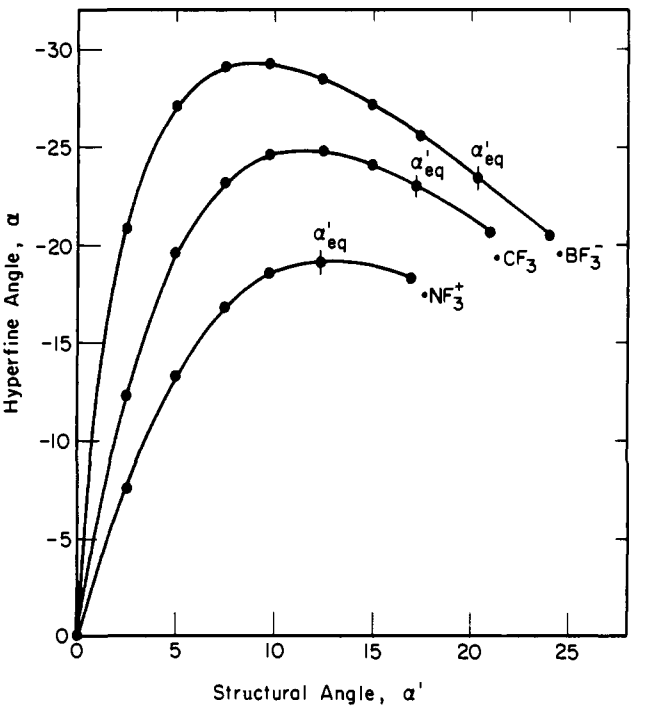

Figure 2. Computed hyperfine angle (α) vs. structural angle (α'), each at DZ level with bond lengths held at equilibrium value. Angles at the potential minima are indicated as α'_{eq}.

Partially Occupied Orbital: Spin Density and EPR. Since the molecular calculations were spin-restricted, the spin density is associated entirely with the $6a_1$ single-occupied orbital in the pyramidal species. Figure 1 shows electron (spin) density contour diagrams for that orbital, whose general characteristics are the same for all three radicals. It utilizes a fluorine p_z orbital that is perpendicular to the M–F bond in the planar molecule but tilts severely toward the bond in the pyramidal molecule so as to allow overlap and bonding with the lower lobe of the central atom's p_z orbital. As is clearly seen in Figure 1, the principal axis of the fluorine dipolar hyperfine interaction is essentially that of the fluorine p_z orbital, which is far from the normal to the M–F bond. Perhaps fortuitously, the structural angle, α, and the hyperfine angle, α', turn out to be about the same in magnitude. However, they are opposite in sign. Note that this general result disagrees with the intuitive idea, expressed by Marauni et al.[25] that the principal axes of the fluorine hyperfine coupling are approximately along and perpendicular to the MF bond.[1] The predicted hyperfine angles (Table II) and principal values of the anisotropic parts of the hyperfine coupling matrices (Table IV) agree reasonably well with the experimental results, where available. The agreement is best for $\cdot NF_3^+$. For $\cdot CF_3$, the previous INDO and spin-unrestricted ab initio SCF results[2,26] are semiquantitatively consistent

(25) J. Marauni, C. A. McDowell, H. Nakajima, and P. Raghunathan, *Mol. Phys.* **14**, 349 (1968).
(26) M. Barfield, A. S. Babagi, D. M. Doddrell, and H. P. W. Gottlieb, *Mol. Phys.*, **42**, 153 (1981).

Table IV. Principal Values of Hyperfine Coupling Matrices[a]

	T_{M_x}	T_{M_y}	T_{M_z}	$T_{F_{x'}}$	T_{F_y}	$T_{F_{z'}}$
			$^{14}NF_3^+$			
DZ	−45.03	−45.03	90.05	−129.04	−164.02	293.06
DZ*	−44.90	−44.90	89.80	−129.43	−164.96	294.39
DZ/ZO	−45.48	−45.48	90.96	−140.18	−178.88	319.07
DZ/OC	−45.89	−45.89	91.79	−154.66	−154.66	309.32
EPR[b]	−45.7	−45.7	91.5	−166.7	−186.7	353.3
			CF_3			
DZ	−74.50	−74.50	149.01	−105.32	−123.63	228.95
DZ*	−73.40	−73.40	146.79	−105.17	−123.44	228.61
DZ/ZO	−72.46	−72.46	144.92	−123.91	−141.52	265.43
DZ/OC	−74.23	−74.23	148.47	−119.71	−119.72	239.43
EPR	−92.2[c]	−39.1[c]	131.3[c]	−158.2[d]	−177.9[d]	336.2[d]
			BF_3^-			
DZ	−47.25	−47.25	94.50	−66.30	−73.34	139.63
DZ*	−42.76	−42.76	85.51	−62.31	−69.02	131.33
DZ/ZO	−42.87	−42.87	85.74	−81.39	−86.99	168.38
DZ/OC	−45.11	−45.11	90.21	−73.02	−73.07	146.08

[a] All entries in MHz. DZ, DZ*, ZO, and OC defined in Table II. [b] From ref 1. [c] From ref 25. [d] From: M. T. Rogers and L. D. Kispert, *J. Chem. Phys.*, 46, B193 (1967).

with our results. For $\cdot BF_3^-$, very nice isotropic EPR spectra have been reported,[27] but anisotropic experimental data are lacking; these calculations provide a pretty good idea of the anisotropic hyperfine interactions to be expected in $\cdot BF_3^-$. Note that only for the anion, $\cdot BF_3^-$, is there a significant effect of diffuse functions on the predicted hyperfine interactions (cf. the preceding section on inversion barriers).

Overlap Spin Density. Barfield et al.[26] recently carried out an INDO test calculation of anisotropic hyperfine interactions for CF_3 and other carbon radicals for a fixed, assumed geometry. They found significant contributions from two- and three-center integrals and from the spin density arising from overlap of atomic orbitals on different centers. To examine this, we recalculated the anisotropic hyperfine interactions at the DZ level, deleting all contributions from two-center overlap spin density. The results, denoted "zero overlap" in Table IV, do indeed show very significant effects for the fluorine interactions. It is remarkable that restoration of two-center overlap density to the INDO wave functions apparently improved the agreement with experiment, while deletion of two-center overlaps from ab initio wave functions had the same effect. The only justification we can offer for downgrading multicenter contributions is that the basis set, being limited, may not have sufficient flexibility to represent the anisotropy in spin distribution very near the fluorine nucleus; the multicenter contributions, which involve the radial tails of the basis functions, should be most susceptible to such an effect. In any case, only the one-center contributions seem to be important for the central atom (see Table IV).

(27) R. L. Hudson and F. Williams, *J. Chem. Phys.* **65**, 3381 (1976).

Table V. Atomic Populations (s:p Character)

	unpaired electron			M–F bond		
	$\cdot NF_3^+$	$\cdot CF_3$	$\cdot BF_3^-$	$\cdot NF_3^+$	$\cdot CF_3$	$\cdot BF_3^-$
DZ	$sp^{6.70}$	$sp^{2.13}$	$sp^{1.18}$	$sp^{2.45}$	$sp^{3.40}$	$sp^{4.54}$
DZ/ZO	$sp^{4.03}$	$sp^{1.30}$	$sp^{0.79}$	$sp^{2.74}$	$sp^{4.31}$	$sp^{5.80}$
EPR	$sp^{6.35}$	$sp^{2.96}$		$sp^{2.47}$	$sp^{3.01}$	

The spin density arising from overlap of atomic orbitals on different centers also has a significant effect on atomic orbital populations. It is interesting that the trend set by inclusion of multicenter contributions in the calculation of the anisotropic hyperfine matrices is reversed for atomic orbital populations; i.e., deletion of two-center overlap appears to improve the agreement with experiment for hyperfine matrices but lowers the correlation for the atomic populations (see Table V). These discrepancies point up the oversimplifications involved in the customary methods of extracting orbital populations from anisotropic EPR data.

The dipolar hyperfine interactions were also recalculated without any inclusion of basis functions centered on other atoms; the results are denoted "one-center", or OC, in Tables II and IV. We see that the principal change is to bring the calculated fluorine hyperfine coupling angles (α') into nearly perfect agreement with the experimental ones. Possibly, this effect originates in our failure to include fluorine 2p basis functions with tight inner loops, so that the one-center contributions are not as great as they should be. Additional calculations with a much larger basis set may test this point and also permit meaningful calculation of isotropic (contact) hyperfine coupling, which we think should not be computed and discussed until more compressed s-type basis functions are included.

Relationship between Structural and Hyperfine Angles. The question arises whether one can get any useful structural information from the orientation of the principal axis of the fluorine hyperfine interaction. To test this, we carried out a series of DZ calculations in which the umbrella angle (α') for each radical was varied (at fixed bond distance) and the hyperfine angle (α) was computed. The curves of α vs. α' for $\cdot NF_3^+$, $\cdot CF_3$, and $\cdot BF_3^-$ are quantitatively different but qualitatively similar. Not only is the hyperfine angle not proportional to the structure angle, but the relationship is not even monotonic. In the case of $\cdot NF_3^+$, the extremum in α vs. α' occurs near the equilibrium geometry. Consequently, the hyperfine angle is not very sensitive to the structural angle in this region. In the other cases, the equilibrium geometry is well past the extremum. The implication is that there is no generally useful relationship between α and α'.

Acknowledgment. This work was supported by grants from the National Science Foundation, Quantum Chemistry Program. We thank Dr. Ira B. Goldberg of Rockwell International Science Center, Thousand Oaks, CA, for stimulating our interest in this problem.

Registry No. $\cdot NF_3^+$, 54384-83-7; $\cdot CF_3$, 2264-21-3; $\cdot BF_3^-$, 37352-52-6.